D. Heinemann*, A. Keller, and D. Jannek

Experimental computer tomograph

Investigation and implementation of iterative reconstruction techniques and modern computer technology

Abstract: The computed tomography is one of the most important medical instruments, allowing the non-invasive visualization of cross sections which are free from superpositions. Since 2000 an experimental computer tomograph of the third generation for the purpose of education and research was set up and further developed. Besides the mechanical construction design reconstruction algorithms, including certain corrections of the measured data were developed and implemented. In 2013 iterative reconstruction methods were investigated and implemented for advanced reconstructions and dose reduction using various ray tracing algorithms. The new reconstruction technique leads to improvements in image quality and low dose reconstructions.

Keywords: computed tomography; filtered backprojection; iterative reconstruction; dose reduction; image quality; CUDA; OpenMP

DOI: 10.1515/CDBME-2015-0072

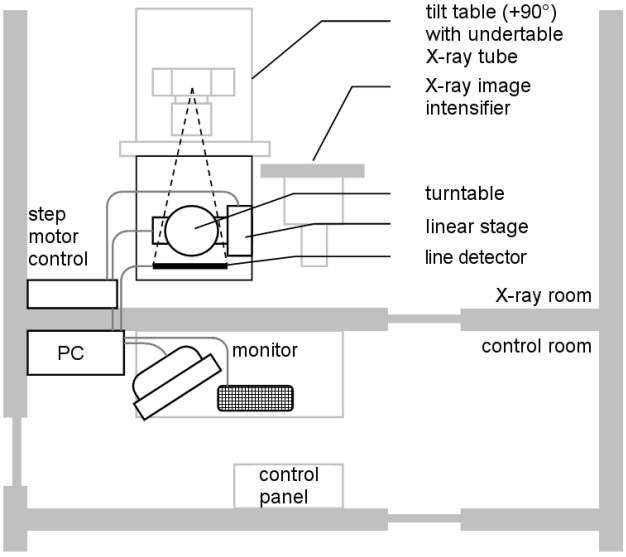

Figure 1: Components and setup of the experimental CT

1 Experimental CT

The computer tomograph of the Institute for Biomedical Engineering and Informatics is an inverse third generation. While the original third generation CTs have a rotary gantry, our system is designed with a turntable, where the examined object is placed between a fixed source-detector-arrangement (see Figure 1). This design reduces the mechanical construction effort, while preserving the basic principle of the third CT generation. Using a linear stage the turntable can be moved vertically through the acquisition geometry. This allows for multiple slice or spiral acquisition for 3D reconstructions. As the detector an industrial X-ray sensible CCD line with optimal quantum efficiency, high spatial resolution, stability of measured data over large acquisition periods and calibration possibilities is used. Due to the system geometry objects with a maximum diameter of 200 mm can be measured and reconstructed. The detector has a spatial resolution of 5 lp/mm, a sensitivity range of 40-160 keV and a sensitive detector length of 214 mm. The measured raw data has a range of values from 0 to 4095 which corresponds to a dynamic range of 12 bit. The resulting sinogram has to be normalized since the raw data represents just an intensity distribution. The correction is based on the attenuation law:

$$I_{corr} = -ln\frac{I}{I_0}. \quad (1)$$

Each intensity value of the detector is corrected by this formula, where I_0 is the intensity of the unattenuated radiation. In consequence of the low-pass characteristic the simple backprojection has to be extended by filtering the projection data, thus the filtered backprojection is obtained for image reconstruction. More detailed information about the system and its behaviour are given in [1–6].

***Corresponding Author: D. Heinemann:** Institute for Biomedical Engineering and Informatics, Technische Universität Ilmenau, Gustav-Kirchhoff-Straße 2, 98693 Ilmenau, Germany, E-mail: david.heinemann@tu-ilmenau.de
A. Keller, D. Jannek: Institute for Biomedical Engineering and Informatics, Technische Universität Ilmenau, Gustav-Kirchhoff-Straße 2, 98693 Ilmenau, Germany

2 Iterative reconstruction and hardware acceleration

Iterative reconstruction techniques are as old as the computed tomography itself. Due to restrictions in computer technology they were not practical used over the last decades. Recent developments made these techniques more and more applicable. Since 2009 they can be found in the clinical environment for X-ray computed tomography.

2.1 Gereral advantages

One of the most important reasons for using iterative reconstruction techniques is the optimization of diagnostic relevant image information and patient dose. Using the filtered backprojection image noise and dose are interrelated via a so called “root-factor”. While doubling the dose, the noise is only reduced by the square root of 2. If the half of the noise should remain, then the dose has to be 4 times greater. Iterative methods are able to undock the noise from the spatial resolution and can reduce the dose while maintaining or even enhance the image quality und thus the diagnostic relevance.

2.2 Iterative reconstruction with the experimental CT

The basic principle of iterative reconstruction methods can be seen in Figure 2 and consists of a simulation of the measuring process by calculating synthetic projection data. Comparing the synthetic sinogram with original projection data delivers an error between those datasets. Using this error the initial reconstruction is corrected. This step is weighted by a relaxation parameter which controls the convergence of the method. The obtained error in radon space between synthetic and original data can be used for image correction. This can easily be done by using the simple backprojection with the error data. To calculate this error data the synthetic sinogram has to be created. The synthetic projections are the result of specific ray tracing algorithms. A simple and a more accurate version are described in the following sections. The calculation of synthetic data and image correction is performed in loops, thus the iterative methods are more computationally intensive as the simple or filtered backprojection.

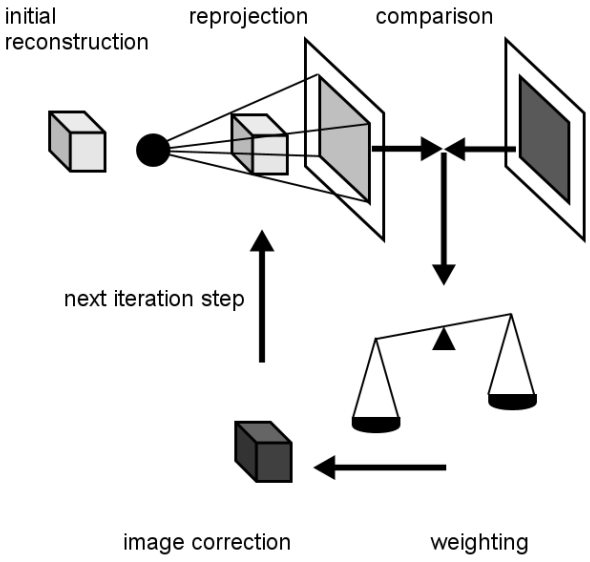

Figure 2: Basic principle of iterative reconstruction

2.2.1 Simple ray tracing

This version of ray tracing does not consider a ray between X-ray source and detector but rays between source and image pixels. Each ray defines a detector element where the current pixel value gives a contribution to (see Figure 3). Via geometric considerations the position of the detector element can be calculated using the formula:

$$t = t_h + \frac{R}{FOD - X} \cdot FDD \tag{2}$$

FOD defines the focus-object-distance, FDD the focus-detector-distance, R describes the distance between pixel midpoint and normal beam, while X determines the distance from the center of rotation to the perpendicular of the current pixel to the normal ray and t_h is the half of the detector length. These variables get different values for each projection angle φ :

$$R(x_a, y_a, \varphi) = R_1 + R_2 = \cos(\varphi) \cdot y_a + \sin(\varphi) \cdot x_a \tag{3}$$

$$X(x_a, y_a, \varphi) = X_1 - X_2 = \cos(\varphi) \cdot x_a - \sin(\varphi) \cdot y_a \tag{4}$$

Inserting these expressions in the formula above one obtains:

$$t = t_h + \frac{(\cos(\varphi) \cdot y_a + \sin(\varphi) \cdot x_a) \cdot FDD}{FOD - (\cos(\varphi) \cdot x_a - \sin(\varphi) \cdot y_a)} \tag{5}$$

Subsequent the current pixel value is added to the detector element value at position t.

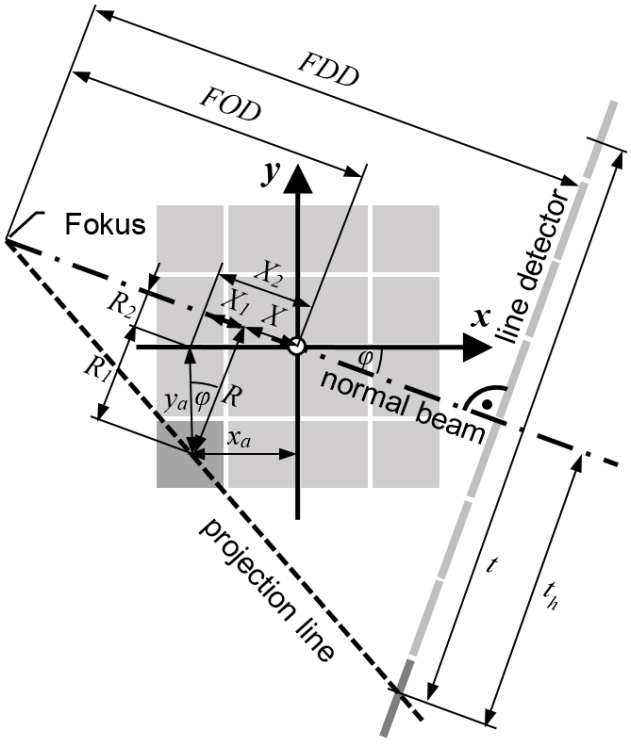

Figure 3: Simple ray tracing

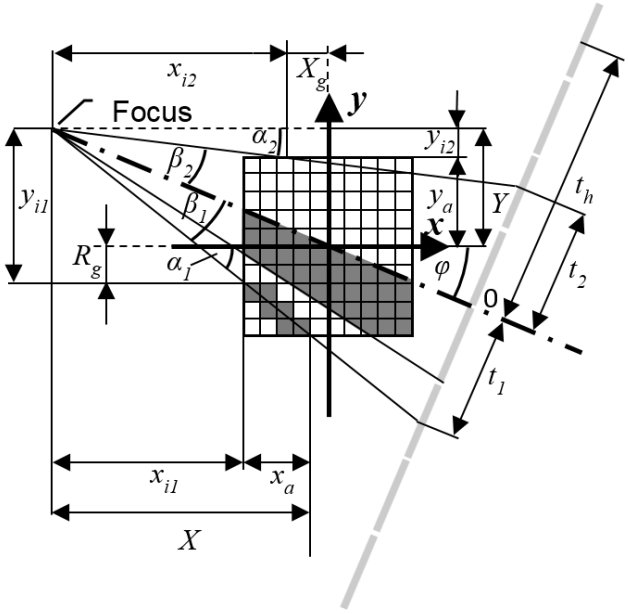

Figure 4: Exact ray tracing

2.2.2 Exact ray tracing

This more accurate version simulates rays from the source to the detector and calculates the pixels which influence the detector value (see Figure 4). At the beginning the entrance point of the projection ray into the image is calculated. x_a holds the value of the left image border if the ray hits the image at this edge and R_g describes whether the ray intersects the upper or the lower half of the image. Due to the consideration of one certain detector element, t_1 is known. The projection rays deflection with respect to the normal ray and to the x-axis is described as:

$$\beta_1 = \arcsin\left(\frac{t_1}{FDD}\right) \text{ and } \alpha_1 = \varphi - \beta_1 \tag{6}$$

Through the knowledge of the spatial source position (X, Y) the exact intersection of the ray can be determined:

$$X = \cos(\varphi) \cdot FOD \text{ and } Y = \sin(\varphi) \cdot FOD \tag{7}$$

$$R_g = Y - y_{i1} \tag{8}$$

$$y_{i1} = \tan(\alpha_1) \cdot x_{i1} \text{ and } x_{i1} = X - x_a \tag{9}$$

The ray intersects the image at the left border if y_{i1} is between the upper and lower image border. If not the next boarder is checked and X_g is examined. The calculations of α_2 and β_2 are analogous.

$$X_g = X - x_{i2} \tag{10}$$

$$x_{i2} = \tan(\alpha_2) \cdot y_{i2} \text{ and } y_{i2} = Y - y_a \tag{11}$$

Through additional knowledge of pixel size and resolution the first intesected pixel can be determined. Starting from this pixel the projection ray is followed and the values are added to the corresponding detector element, weighted by the length of the projection ray in each pixel. Using this weighting causes a slight error in the reprojected data. As Figure 4 shows only pixels on the projection ray influence the detector value and pixels between rays are missed. This problem can be solved by using area weights like the large dark area in Figure 4.

2.3 Reconstruction using hardware acceleration

The simple sequential processing gives a proper opportunity to compare old and modern computer technology. In the previous version of the reconstruction computer an AMD XP 2200 processor (1 x 1.8 GHz) was installed, while the current system uses an Intel Core i7 950 (4 x 3.07 GHz). The systems deliver a processing time of 50 seconds for the old and 3 seconds for the modern system. As a first real acceleration method OpenMP is used. OpenMP (Open Multi-

Processing) gives the opportunity to run code on all available CPU cores in parallel. By parallelizing all for-loops the processing was accelerated by 40 %. **NVIDIAs CUDA** is used to create high performance reconstructions. Modern graphics cards have hundreds of processing units which operate in parallel. The code was designed in such a way that each processing unit of the graphics card runs calculations for only one pixel. By using this technology the reconstruction was done in 42 milliseconds. This means an acceleration by the factor 1190.

3 Results

We acquired a phantom (see Figure 5) with four radiation doses. The acquisition parameters where 100 kV, 1.5 mA. Varying the integration time (0.05 ms; 0.1 ms; 0.15 ms; 0.2 ms results in dose reductions of 25 %, 50 % and 75 %. Figure 5 shows reconstructions with 25 % (first row) and 100 % (second row) dose using the filtered backprojection (left) and the developed iterative reconstruction (right). As mentioned in the previous section the noise directly corresponds with the applied dose what can clearly be seen in Figure 5. The first row shows a significant worse image quality due to increased noise. Using the iterative method the image noise is reduced and spatial resolution is maintained. Even a dose reduction of 75 % gives a better reconstruction result as the filtered backprojection with 100 % dose. Variations of the acquired data and reconstructions obtained from certain parameter settings of the iterative algorithms are demonstrated in [7].

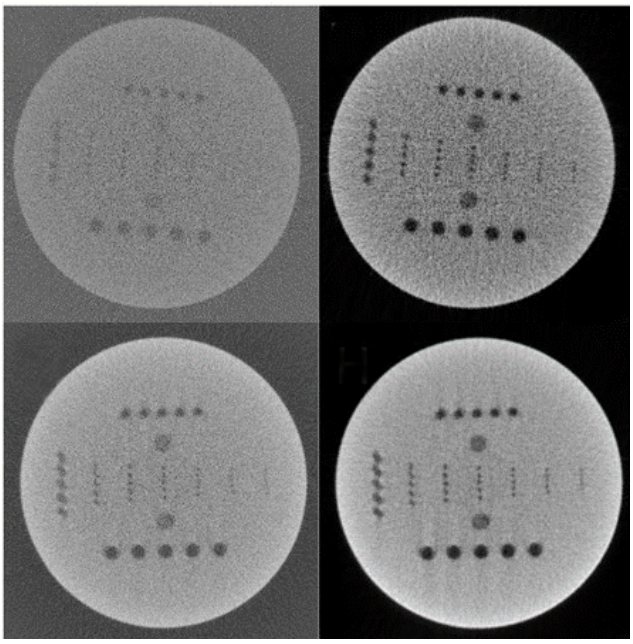

Figure 5: Reconstructions with different doses

4 Conclusion

The investigated algorithms and the implementation extend the experimental CT with respect to modern reconstruction techniques and technology. This gives forward looking opportunities in education and research in the field of computed tomography. Even with much lower radiation dose the reconstruction with consistent or better image quality is possible. Significant acceleration of the processing was reached by using modern computer technology. The software and algorithms are still under further development and will give additional improvements in future work.

Author's Statement

Conflict of interest: Authors state no conflict of interest. Material and Methods: Informed consent: Informed consent is not applicable. Ethical approval: The conducted research is not related to either human or animals use.

References

[1] Keller A.: Experimenteller Computertomograph für Ausbildung und Forschung – Teil 1: Modellierung der Querschnittsrekonstruktion. In: medizintechnik 2002 (3), 122: 103–105.
[2] Gross S., Keller A., Krüger U.: Experimenteller Computertomograph für Ausbildung und Forschung – Teil 2: Problemanalyse, Konzept, Bildrekonstruktion. In: medizintechnik 2002 (4), 122: 135–140.
[3] Kyriakou Y., Keller A.: Experimenteller Computertomograph für Ausbildung und Forschung – Teil 3: Aufhärtungskorrektur. In: medizintechnik 2004 (1), 124: 15–19.
[4] Keller A., Scholz N., Schmidt F.: Experimenteller Computertomograph für Ausbildung und Forschung – Teil 4: Örtliche Dynamik des Zeilendetektors. In: medizintechnik 2005 (4), 125: 131–137.
[5] Keller A., Heinz Chr.: Experimenteller Computertomograph für Ausbildung und Forschung – Teil 5: Schwächungsmessung, CT-Zahlen. In: medizintechnik 2007 (2), 127: 71–75.
[6] Keller A., Herzog S.: Experimenteller Computertomograph für Ausbildung und Forschung – Teil 6: Erfahrungen und Ergebnisse. In: medizintechnik 2011 (6), 131: 224-228.
[7] Heinemann D.: Methodischer Vergleich iterativer Rekonstruktionsverfahren bei der Computertomographie, Master Thesis, Technische Universität Ilmenau 2013: 160.